DESIGN AND EXPERIMENTAL RESEARCH OF SELF-PROPELLED TOBACCO STEM HARVESTER

/

自走式烟杆收获机设计与试验研究

Liquan YANG[1,2], Guangyu YIN[1,2], Rui FENG[1], Junya HUANG[1], Xiaodong LIU[1], Jianbo WANG[1], Dongwei YAN[1], Qingqing Lü[1, *], Guangxi LI[1, *]

[1] Henan Province Engineering Research Centre of Ultrasonic Technology Application, Pingdingshan University, Pingdingshan, Henan 467000, China

[2] Pingdingshan Company, Henan Tobacco Company, Pingdingshan, Henan 467000, China

** Corresponding author: Qingqing Lü, Guangxi LI*

Tel: +8618339975718; E-mail: 2696@pdsu.edu.cn, 2677@pdsu.edu.cn

DOI: https://doi.org/10.35633/inmateh-79-06

Keywords: *Self-Propelled, Tobacco Stem Harvester, SolidWorks, ANSYS Simulation, Field Experiment*

ABSTRACT

To promote the mechanization of the tobacco industry, a self-propelled tobacco stem harvester was designed in this study. To improve harvesting efficiency under varying terrain and planting conditions, the machine integrates key functional components, including a chain-clamp conveyor and a loosening shovel with optimized structural parameters. The performance of these core components was analysed using 3D modelling and finite element simulations conducted in ANSYS. Field experiment optimization indicated that the optimal operating parameters were a clamping chain speed of 0.7 m/s, a forward travel speed of 0.4 m/s, and a clamping chain gap of 12 mm. Experimental results showed that the harvester achieved a leakage rate of 3% and a breakage rate of 7%. Overall, the machine demonstrated reliable performance and satisfied practical operational requirements. This study provides an effective technical solution for the mechanization of tobacco stem harvesting, contributing to reduced production costs and the advancement of agricultural modernization.

摘要

为推进烟草产业机械化发展，解决烟杆后处理机械化清理的难题，设计了一种自走式烟杆收获机，针对不同地形及种植条件，旨在提升烟杆收获效率。采用 SolidWorks 三维建模、Ansys 有限元仿真和 Adams 运动分析软件，设计并优化了松土铲、链夹式夹持输送链、粉碎刀辊等核心零部件。为验证烟杆收获机的作业性能，以烟杆漏拔率和拔断率为试验目标，设计了单因素试验和正交试验进行了田间测试，综合分析结果表明夹持链运动速度 0.7m/s、机器前进速度 0.4 m/s、夹持链间隙 12 mm 时综合作业效果最佳，收获漏拔率 3%、拔断率 7%，烟杆粉碎后颗粒长度主要集中在 40-50mm，作业性能优良，满足使用需求。本研究为烟杆收获机械化提供了可行的技术方案，对降低生产成本、促进农业现代化具有重要意义。

INTRODUCTION

Tobacco is one of the world's most important cash crops *(Zeng et al., 2024; Mo, 2023; Wu, 2007)*, particularly in Asia, Africa, and South America, where many countries' economies rely heavily on the tobacco industry *(Zhang, 2016)*. As the world's largest producer and consumer of tobacco, China plays a significant role in generating farmers' income and local economic development through tobacco cultivation. Tobacco stems and roots are the residues left after tobacco leaf harvesting *(Yang et al., 2015).* Due to their high lignin and cellulose content, they provide an ideal overwintering site for harmful microorganisms, such as bacteria and viruses, serving as hosts for various pathogens *(Li et al., 1999)*. They cannot be used as fertilizers for on-site application *(Zhang, 2007)*; therefore, they must be promptly removed from tobacco fields. Tobacco roots are large in volume and tightly bound to the rhizosphere soil, making them difficult to remove completely *(Li et al.,2010)*. After tobacco leaf harvesting each year, many tobacco stems and roots are discarded in fields, ditches, or riverbanks, forming agricultural waste that pollutes the soil and severely impacts the development and growth of the next crop season *(Zhang, 2007; Li, 2009; Reynaldo et al., 2000; Jin et al.,1999).* Manual collection of tobacco stems and roots faces issues such as high labour intensity and low collection efficiency. Existing tobacco stem removal machinery primarily uses counter-rotating blades to remove stems and roots, which can cause root system fractures and severe residue problems. Therefore, an efficient tobacco field root removal mechanism is urgently required to address these issues *(Tu, 2006)*.

Some developed countries, such as the United States, France, and Japan, have been at the forefront of research into tobacco stem cleaning machinery, with advanced technology and rapid development *(Guo et al., 2023)*. These machines are characterized by multi-functionality, high power, and high levels of integration. However, their large size and working width render them unsuitable for the small-scale cultivation practices of Chinese tobacco farmers. Domestic machinery in China is mostly single-function, primarily designed for stem removal, with few machines capable of integrating functions such as stem removal, transportation, crushing, and collection.

Therefore, this study designed a self-propelled tobacco stem harvester capable of simultaneously completing tobacco stem pulling, root removal, transportation, and crushing operations, effectively addressing the issues of single functionality and low mechanization levels in existing tobacco stem cleaning equipment. Kinematic and dynamic analyses, finite element simulations, and field trials were conducted on the mechanism.

MATERIALS AND METHODS

1. Overall structural design of the self-propelled tobacco stem harvester

The self-propelled tobacco stem harvester completes the tasks of deep loosening of tobacco roots, pulling up tobacco stems, conveying, crushing, and collecting in a single operation. The main transmission system of the machine primarily uses a chain drive and gear meshing transmission. Power is provided by two 74-horsepower engines, one for machine movement and the other for the pulling stem operation. Based on the overall structural and functional requirements, the lifting arm assembly was designed at a 45° angle to the horizontal ground, with the initial clamping position set at 60° to enhance contact between the tobacco stems and conveyor chain and reduce the risk of missed lifting. Twelve bearing mounting sleeves were symmetrical welded to the outer side of the conveyor chain, providing stable pulling power through the gear transmission system. The integrated soil-loosening blade structure at the front significantly reduced the pulling force required to lift the tobacco stems. Additionally, the inner side of the clamping chain is equipped with a spring-loaded clamping mechanism that dynamically adjusts the gap between the two chains through elastic deformation, ensuring reliable clamping of the tobacco stems during lifting and effectively preventing slippage. The overall structural design is illustrated in Fig. 1.

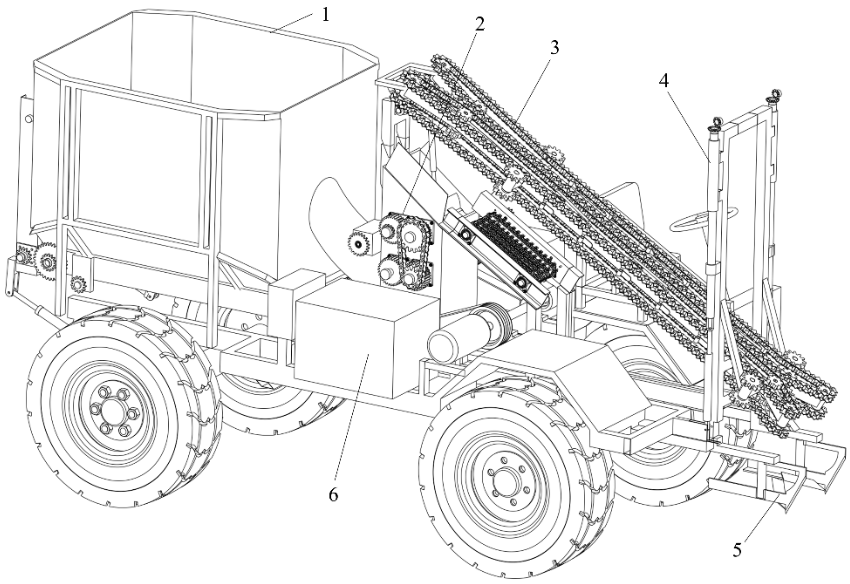

Fig. 1 – Structural diagram of a self-propelled tobacco pole harvester

1. Material-receiving hopper 2. Crusher 3. Clamping chain 4. Lifting hydraulic cylinder 5. Soil loosening blade 6. Engine

1.1. Overall design of clamping conveyor chain

The clamping stem mechanism *(Gao et al., 2025)* rotates counterclockwise under the drive of the drive wheel, conveying the clamped tobacco stems to the crusher for crushing them. Although the clamping-type conveying method uses elastic components to secure tobacco stems, they may slip or shift during conveying, leading to blockages. Considering that tobacco stems ultimately need to be shredded and returned to the field, there is no need to maintain their original shape. After a comprehensive comparison and analysis, this study selected a chain-clamping stem device as the core conveying structure to ensure the stability of tobacco stem conveyance and operational continuity.

To ensure that the clamping chain maintains a stable clamping force and efficient transmission performance during tobacco stem conveying, an internal tensioning wheel staggered layout design was adopted, with external tensioning wheels installed to effectively avoid clamping force reduction and derailment risks caused by chain elongation. By welding U-shaped brackets to the top of both side supports, the structural integrity was enhanced to prevent component separation. To address the complex terrain of tobacco fields, bearings were installed in the bearing brackets, and a hydraulic cylinder was integrated at the front end of the clamping mechanism. These two components work in tandem to achieve dynamic height adjustment of the lifting stem assembly, thereby enhancing the environmental adaptability of the equipment. The power transmission mechanism is as follows: the universal joint driveshaft transmits power to the drive sprocket, driving the driven sprocket to rotate in the counterclockwise direction. After the tobacco stems are loosened by the soil loosening blade, they are fed into the clamping and pulling stem device inlet, immediately clamped by the clamping chain, and pulled out of the soil. Under the coordinated action of the tensioning wheels, the tobacco stems were smoothly conveyed to the shredding device inlet, as shown in Fig. 2.

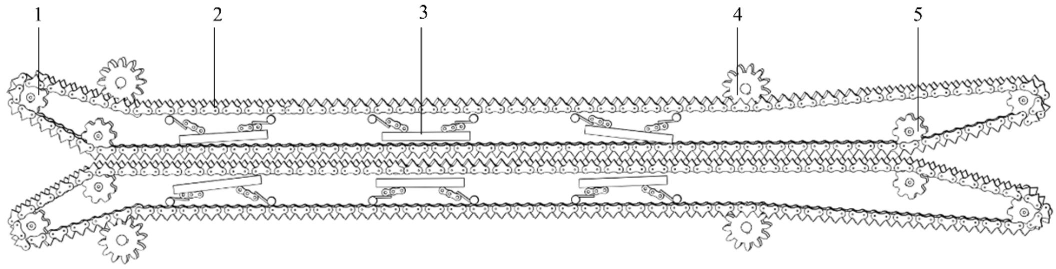

Fig. 2 – Clamping chain structure

1. Drive sprocket 2. Clamping chain 3. Clamping plate 4. External tension sprocket 5. Gap adjusting sprocket

1.2. Loosening Shovel Design

Loosening shovels can be classified into chisel-, arrow-, and wing-shaped shovels *(Fan, 2022)*, duck-foot shovels, vibrating loosening shovels, and combination shovels. Based on the soil type of the tobacco field, a combination shovel type was selected to adapt to different working environments. According to the research findings in *Yu et al., (2007), and Tong et al., (2005)*, the operational resistance of a soil loosening shovel is primarily influenced by factors such as shovel type, operational speed, operational depth, and angle of penetration. Because the shovel structure and operational speed were already finalized in this study, the research focus was on determining the operational depth and angle of penetration parameters of the soil loosening shovel.

(1) Working depth

The appropriate selection of working depth is crucial for reducing working resistance, protecting the soil structure, and ensuring operational effectiveness. Excessively deep working depths increase the working resistance, leading to higher energy consumption, component wear, and damage to the soil's original aggregate structure. Conversely, excessively shallow depths do not meet the operational requirements for effectively loosening tobacco stems. According to relevant research *(Guo, 2023),* when the working depth is between 200 and 300 mm, effective loosening can be ensured while balancing energy consumption and soil protection. After careful consideration, this study selected 250 mm as the working depth of the loosening blade to achieve a balanced optimization of the working performance and energy consumption.

(2) Angle of Entry

The size of the angle of entry directly affects the ease of entry of the loosening blade *(Zhang 2014)*. An excessively small angle makes penetration difficult and reduces work efficiency, whereas an excessively large angle increases resistance and accelerates tool wear. According to the literature *(Wang et al., 2007)*, the optimal penetration angle is 60°–70°; therefore, 60° was selected.

After determining the parameters, the tillage blade was modelled, as shown in Fig. 3.

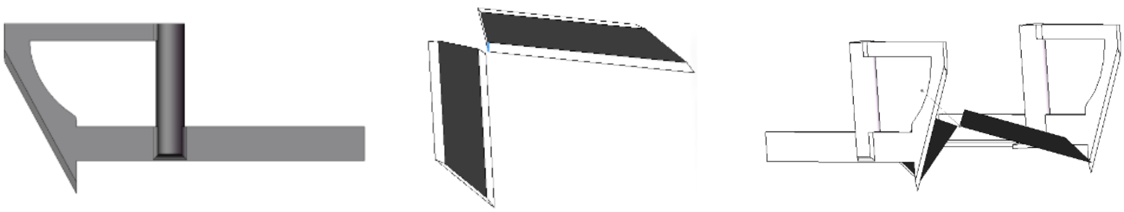

(a) Shovel frame (b) Shovel blade (c) Assembly

Fig. 3 – General assembly drawing of ripper shovel

1.3. Analysis of the dimensions of the crushing roller

The tobacco stem *(Chen et al., 2025)* was crushed using a multi-roller crusher *(Jiang et al., 2019)*, and the model and spatial arrangement of the roller are shown in Fig. 4.

(a) Knife roller model (b) Four knife roller arrangement configurations

Fig. 4 – Knife roller model and its arrangement

According to *Yang et al., (2024)*, the cutting speed of tobacco stems is generally between 16 and 30 m/s. The diameter of the cutting roller was 240 mm, and the minimum cutting speed of the cutting roller was:

$$n_{\min} = \frac{30v}{\pi R} = \frac{30 \times 14}{\pi \times 0.24} = 557\ \mathrm{r \cdot min^{-1}} \tag{1}$$

where: $n_{\min}$ is the minimum cutting speed of the cutting roller, r·min^{-1}; v is minimum linear velocity, m·s^{-1}.

Maximum cutting speed:

$$n_{\max} = \frac{30v}{\pi R} = \frac{30 \times 30}{\pi \times 0.24} = 1193.7\ \mathrm{r \cdot min^{-1}} \tag{2}$$

where: $n_{\max}$ is the maximum cutting speed of the cutting roller, r·min^{-1}; v is maximum linear velocity, m·s^{-1}.

The rotational speed of the cutting roller was selected as 800 r·min^{-1}.

According to the Agricultural Machinery Design Manual *(Wang et al., 2007)*, the relationship is expressed as follows:

$$H = d + \frac{r v_m}{v_d} \tag{3}$$

where: H is the distance between the knife holder and the centre of the spindle, mm; d is the diameter of the tobacco stem, mm; r is the rotation radius of the cutting roller blade, mm; v_m is the conveying speed of the conveyor chain, m·s^{-1}; v_d is the linear speed of the cutting roller blade, m·s^{-1}.

1.4. Design of the Transmission System for the Tobacco Stem Harvester

The self-propelled tobacco stem harvester's transmission system uses a combination of chain and belt drives. The output shaft of the main motor transmits power to the transfer case, which is then distributed by gear z1 to the symmetrically arranged bevel gears z2 and z3 on both sides. The bevel gears drive the clamping chains at equal speeds in opposite directions, thereby providing the required power for tobacco stem clamping. Auxiliary motor 2 transmits power via a belt drive to gear z8, which subsequently drives z10, z11, and z12. These four gears operate in coordination to realize the synchronous counter-rotation of the four cutting rollers, as shown in Fig. 5.

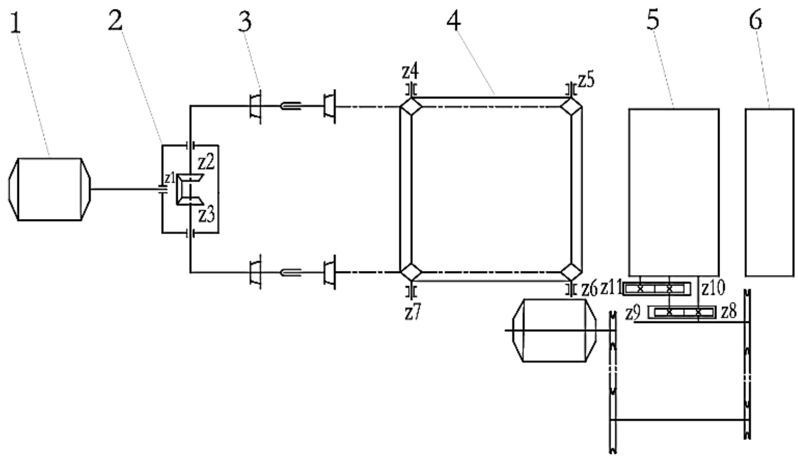

Fig. 5 – Transmission system of the tobacco harvester

1. Motor 2. Transfer case 3. Universal drive shaft 4. Clamping chain 5. Crushing device 6. Collection bin

1.5. Design of the Hydraulic System for the Tobacco Stem Harvester

To enable the tobacco stem harvester to adapt to varying field terrain conditions, two hydraulic cylinders were installed on both sides of the clamping chain. When operating on elevated terrain, the clamping chain can be raised, whereas on lower terrain it can be lowered accordingly, ensuring efficient and accurate tobacco stem harvesting. The hydraulic system mainly consists of a hydraulic pump, a relief valve, a three-position four-way directional control valve, and a check valve, as shown in Fig. 6.

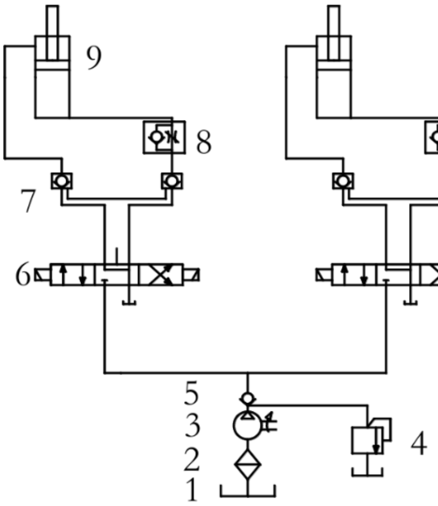

Fig. 6 – Hydraulic system of tobacco stem harvester

1. Oil tank; 2. Filter; 3. Hydraulic pump; 4. Relief valve; 5. Check valve; 6. Three-position, four-way directional control valve; 7. Pilot-operated check valve; 8. Throttle check valve; 9. Hydraulic cylinder

Hydraulic pump *3* serves as the power source of the system, supplying pressurized hydraulic oil and constituting the core of the hydraulic system. Hydraulic cylinder *9* acts as the actuator, converting hydraulic energy into mechanical energy to drive the movement of the working components. Relief valve *4*, check valve *5*, control check valve *7*, throttle check valve *8*, and the three-position four-way directional control valve *6* function as control and regulating components, governing the pressure, flow rate, and flow direction of the hydraulic oil. Oil tank 1 and filter *2* are auxiliary components that ensure reliable and stable system operation. During operation, hydraulic oil stored in oil tank *1* is filtered by filter *2* and then drawn in and pressurized by hydraulic pump *3*. The pressurized oil passes through check valve *5*, which prevents reverse flow, and enters the directional control valve *6*. By switching positions, the directional control valve controls the flow direction of the hydraulic oil. When the valve is set to the corresponding working position, the pressurized oil flows through its internal passages, passes through control check valve *7*, and enters either the rodless chamber or the rod chamber of hydraulic cylinder *9*. The piston extends when oil enters the rodless chamber and retracts when oil enters the rod chamber. The throttle check valve *8* regulates the flow rate of the hydraulic oil entering and leaving the hydraulic cylinder, thereby controlling the piston movement speed. Relief valve *4* limits the system pressure; when the pressure exceeds the preset value, the valve opens to return oil to the tank, ensuring system safety.

2. Stress Analysis and Motion Simulation of Key Components

2.1. Force analysis of deep loosening plough

An Ansys finite element simulation was used to determine the material properties and mesh division for the loosening plough model, and a constraint force of 500 N was applied. The equivalent stress and total deformation cloud diagrams are shown in Fig. 7 and 8, respectively.

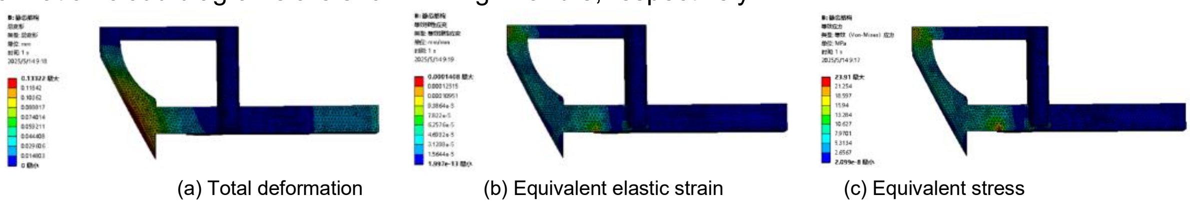

(a) Total deformation (b) Equivalent elastic strain (c) Equivalent stress

Fig. 7 – Stress contour diagram of ripper shovel 1

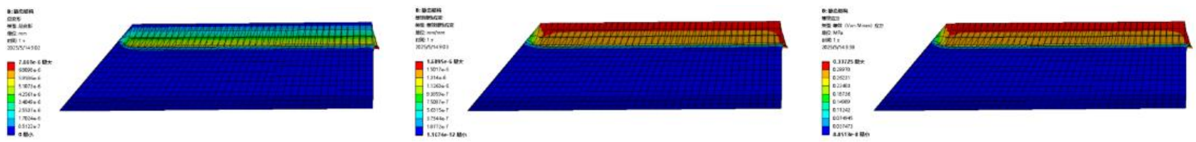

(a) Total deformation (b) Equivalent elastic strain (c) Equivalent stress

Fig. 8 – Stress contour diagram of soil loosening shovel 2

The maximum stress on the soil loosening blade frame during operation was 39.91 MPa, primarily concentrated in the middle and lower sections of the blade edge. This value is significantly below the allowable stress of the material, ensuring structural safety and reliability. Under the influence of operational bending moments, the maximum deformation of the soil loosening blade was 0.13322 mm, which is an imperceptible micro-deformation not visible to the naked eye and does not affect harvesting operations, indicating that the soil loosening blade design meets the requirements. The maximum stress on the soil loosening blade was 0.33725 MPa, and the maximum deformation was 7.661×10^{-6} mm. The maximum stress on the soil loosening blade was far below the material yield strength of 250 MPa, and the deformation was small. Therefore, the design is safe, reliable, and meets operational requirements.

2.2. Simulation of the clamping and pulling stem mechanism

2.2.1. Modelling of the clamping process

The tobacco stem is the main test object, and its parameters significantly affect the final test results. Through research on the physical characteristics of the tobacco stem, it was determined that the length, diameter, and mass of the tobacco stem were approximately 1200 mm, 25 mm, and 695 g, respectively.

The volume of the tobacco stem can be obtained from Equation (4)

$$V=\pi r^2 h=\frac{\pi D^2 h}{4}=\frac{3.14\times 25^2\times 1200}{4}=588.75\ \text{cm}^3 \tag{4}$$

where: V is the volume of the tobacco stem, cm^3; D is tobacco diameter, cm; h is tobacco length, mm.

Using the density formula $\rho = m/v$, the density of the tobacco stem was approximately 1.18 g/cm³. According to *Wang et al., (2007)*, the elastic modulus of the tobacco stem is 1147 MPa, and the Poisson's ratio is 0.33.

During the clamping and pulling processes, owing to the complexity of the simulation process, most components did not significantly affect the simulation results. Therefore, simplifying the model not only provides a more intuitive representation of the motion process but also significantly reduces simulation complexity.

In SolidWorks, components such as the frame, clamping chain, and bearings were simplified, parameters were set, and the model was saved in the '*.xt' file format before being imported into Adams for simulation analysis. The simplified model is illustrated in Fig. 9.

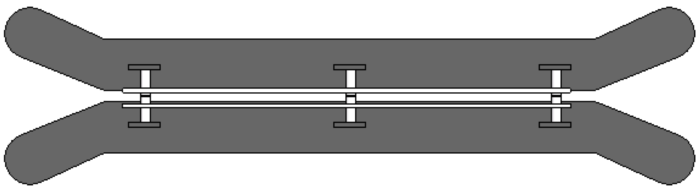

Fig. 9 – Simplified model of the clamping mechanism

The clamping device operates through the coordinated action of various mechanisms, and simulating its motion requires constraints between the mechanisms. Specifically, the operational state of the mechanisms is equivalent to the linear motion of the model, the spring tension state when the tobacco holder is clamped is equivalent to the linear motion of the stopper plate, and the tobacco holder clamping process is equivalent to the linear motion of the tobacco holder. When the tobacco stem is clamped, it comes into contact with the clamping link, thereby generating a contact force. According to reference *(Pu, 2005),* the contact force between the tobacco stem and clamping link is continuous. In the Adams software, the formula for calculating the contact stiffness coefficient K of the object contact system is shown in Equation (5).

$$K=\sqrt{\frac{16RE^2}{9}}=\frac{4}{3}E\sqrt{R} \tag{5}$$

where: R is the contact radius，mm; E is the moment of inertia, MPa.

$$\frac{1}{R}=\frac{1}{R_1}+\frac{1}{R_2} \tag{6}$$

where: R_1 and R_2 represent the contact radius of the object during the contact process. If the contact surface is flat, the contact radius becomes infinite.

$$\frac{1}{E}=\frac{(1-\mu_1^{\ 2})}{E_1}+\frac{(1-\mu_2^{\ 2})}{E_2} \tag{7}$$

where: E_1 and E_2 are the Young's moduli between the two contacting objects，MPa, and μ_1 and μ_2 are the Poisson's ratios between the two contacting objects.

During the simulation process, the material selected for the clamping chain was 45 steel, with a Young's modulus of 2.09 × 10⁵ MPa and Poisson's ratio of 0.269. The Young's modulus of the tobacco stem was 1147 MPa, and the Poisson's ratio was 0.33. The simulated motion of the tobacco stem in Adams is the contact between the tobacco stem and guard plate, which can be regarded as the contact between a cylindrical surface and plane. Based on the modelling of the tobacco stem, the contact radius of the tobacco stem was set to 12.5 mm. Substituting the data into Equations (8) and (9) yields:

$$\frac{1}{R}=\frac{1}{12.5}+\frac{1}{\infty} \tag{8}$$

$$\frac{1}{E}=\frac{(1-0.3^2)}{2.05\times10^5}+\frac{(1-0.33^2)}{1147} \tag{9}$$

Substituting the data into Equation (2) yields the contact stiffness coefficient K:

$$K=\frac{4}{3}E\sqrt{R}=\frac{4}{3}\times1279.9\times\sqrt{12.5}=6033.6 \tag{10}$$

2.2.2. Simulation analysis of the clamping process motion

The simulation analysis of the clamping process motion mainly analyses the displacement, velocity, and acceleration of the tobacco stem as it moves from the lower to the upper end of the clamping chain. The simulation results obtained using Adams software are shown in Figs. 10–12.

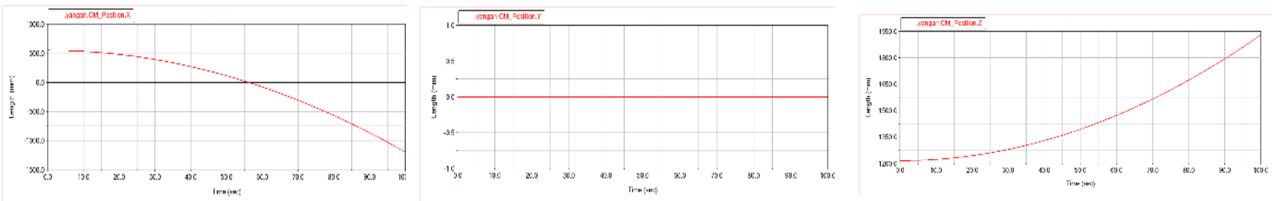

(a) Displacement in the X direction (b) Displacement in the Y direction (c) Displacement in the Z direction

Fig. 10 – Displacement curve of the tobacco holder clamping point

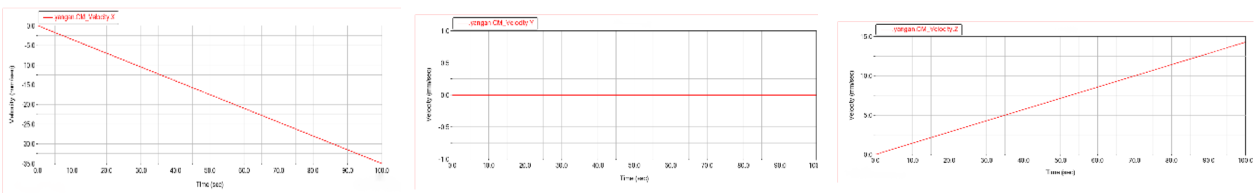

(a) Displacement in the X direction (b) Displacement in the Y direction (c) Displacement in the Z direction

Fig. 11 – Speed curve of the tobacco holder clamping point

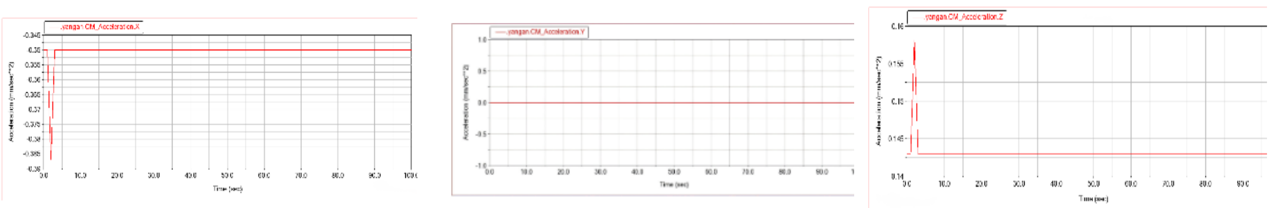

(a) Displacement in the X direction (b) Displacement in the Y direction (c) Displacement in the Z direction

Fig. 12 – Acceleration curve of the tobacco holder clamping point

By analysing the displacement curve shown in Fig. 10, it can be seen that tobacco stem 1 exhibits a negative displacement trend along the X-axis, as the displacement direction is opposite to the positive direction of the coordinate axis, effectively increasing the displacement magnitude; the displacement along the Y-axis remains constant, while the displacement along the Z-axis continues to increase. This result directly reflects the actual operating conditions of the tobacco stem moving backward along the longitudinal (Z-axis) direction under the influence of the conveyor chain after being clamped and pulled out, which is consistent with the theoretical expectations.

Fig. 11 shows that the velocity of the tobacco stem along the X and Z axes increased in opposite directions in a synchronized manner, whereas the velocity along the Y axis remained zero throughout, further validating the directional conveying characteristics of the tobacco stem within a two-dimensional plane.

Fig. 12 indicates that the acceleration along the Y-axis is zero, whereas the acceleration along the X- and Z-axes remains relatively stable during motion, although significant fluctuations occur between 0 and 5 s. The analysis indicates that this fluctuation is caused by an instantaneous change in acceleration due to inertial forces when the smoke stem is lifted. As the smoke stem entered the stable conveying phase, the acceleration gradually returned to a steady state.

Based on the analysis results of the displacement, velocity, and acceleration, the clamping and lifting stem mechanism operated smoothly, and its dynamic performance met the design specifications.

3. Field Trial of Tobacco Stem Harvester

The trial site was selected in the tobacco fields of the Yilong Machinery Factory in Henan Province, using tobacco stems from the current season. The tobacco stems used in the trial were those remaining after tobacco leaf harvesting, with an average height of approximately 1200 mm, an average diameter of 30.6 mm, and plant spacing of 60 mm. The tobacco field ridges were 50 cm wide, 30 cm high, and spaced 80 cm apart from each other. The trial site had no recent rainfall, with clear weather and moderate soil moisture content, which made it suitable for the trial operations.

Typically, mechanical operations require that the rate of harvest omission and the rate of tobacco stem breaking (the roots are not pulled out, but the stems are broken) should both be below 10%. The formulas for calculating the rate of harvest omission (Y_1) and the rate of stem breaking (Y_2) are as follows:

Stem removal performance indicators

$$\text{Harvest omission rate: } Y_1=W_1/W \tag{11}$$

$$\text{Stem breaking rate: } Y_2=W_2/W \tag{12}$$

where: Y_1 represents the rate of tobacco harvest omission, Y_2 represents the rate of tobacco stem breaking, W_1 represents the number of tobacco harvest omissions, W_2 represents the number of broken tobacco stems, and W represents the total number of tobacco stems tested.

The primary operational parameters affecting the tobacco harvest omission and stem breaking rates were the clamping chain transmission speed, harvester forward speed, and clamping chain clearance. These parameters were tested to determine their influence on the tobacco harvest omission and stem breaking rates. The field trial process is illustrated in Fig. 13.

(a) Test process (b) Condition of tobacco fields after testing

Fig. 13 – Field experiments

3.1. Single-factor field test

3.1.1. Effect of clamping chain transmission speed on tobacco harvest omission rate and stem breaking rate

The forward speed of the tobacco-stem harvester can be adjusted using a transmission gearbox. The transmission speed of the dual-row clamping chain was controlled by the drive system, whereas the clamping chain gap was finely adjusted using nuts on the compression springs. In the first field trial, the forward speed of the harvester was set to 0.6 m/s, and the clamping gap was set to 9 mm. Five gradient clamping chain transmission speeds of 0.6, 0.8, 1.2, 1.5, and 1.8 m/s were selected for testing. During the trial, 100 tobacco stems were pulled for each parameter set. The results of the field trials are shown in Fig. 14.

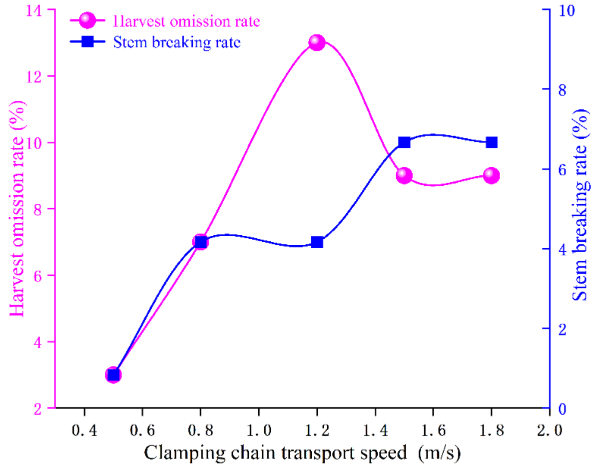

Fig. 14 – The harvest omission rate and stem breaking rate of tobacco stems under different speeds of clamping chain

Fig. 14 shows that when the conveying speed of the clamping chain is within the range of 0.6–1.2 m/s, the leakage rate increases linearly with the speed. However, when the speed increased to 1.2–1.5 m/s, the harvest omission rate decreased slightly and stabilized at 1.5 m/s. The stem breaking rate continued to increase with increasing conveying speed, reaching a peak near 1.5 m/s before stabilizing. Considering the dual optimization requirements of the harvest omission and stem breaking rates, the overall performance of tobacco stem removal was optimal when the conveying speed of the clamping chain was controlled between 0.6 and 0.8 m/s.

3.1.2. Effect of harvester forward speed on tobacco harvest omission rate and stem breaking rate

The conveying speed of the clamping chain was set to 0.7 m/s, and the forward speeds of the tobacco stem harvester were set to 0.4, 0.5, 0.6, and 0.7 m/s, respectively, while maintaining a constant chain gap of 9 mm. A total of 100 tobacco stems were pulled, and the harvest omission and stem breaking rates were recorded. The test results are presented in Fig. 15.

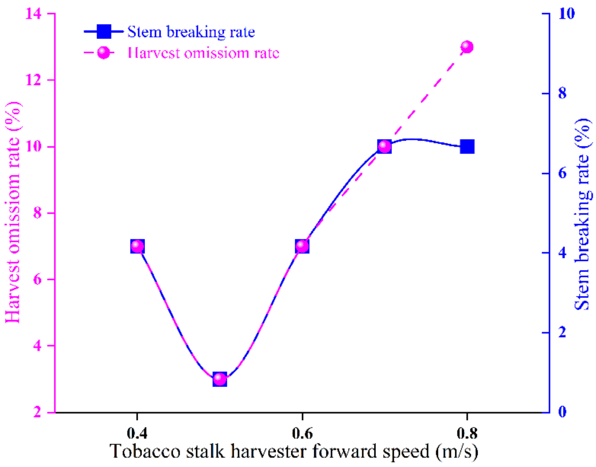

Fig. 15 –The harvest omission rate and stem breaking rate of tobacco stems under different harvester forward speeds

According to the experimental data in Fig. 15, when the forward speed of the tobacco stem harvester was within the range of 0.4–0.5 m/s, the harvest omission rate decreased as the speed decreased.

However, within the range of 0.5–0.7 m/s, the stem breaking rate increased with speed, reaching a peak at 0.7 m/s and then stabilizing. Combining the harvest omission rate and stem breaking rate change curve, within the 0.4–0.5 m/s speed range, the stem breaking rate decreased as speed increased, and within the 0.4–0.6 m/s range, the stem breaking rate showed an upward trend. Through a comprehensive dual-indicator optimization analysis of the harvest omission and stem breaking rates, when the forward speed of the tobacco stem harvester was controlled between 0.4 and 0.6 m/s, the overall operational performance of the equipment reached its optimal level. This parameter effectively reduces the risk of harvest omission and stem breakage while ensuring operational efficiency of the harvester.

3.1.3. Effect of clamping chain spacing on tobacco harvest omission rate and stem breaking rate

The clamping chain conveying speed was set to 0.7 m/s, and the tobacco stem harvester forward speed was set to 0.5 m/s. Clamping chain gaps of 7, 9, 12, 15, and 18 mm were selected. Under these conditions, 100 tobacco stems were pulled, and the harvest omission and stem breaking rates were recorded. The test results are presented in Fig. 16.

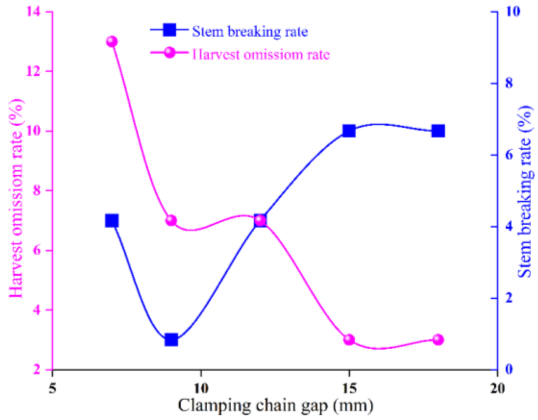

Fig. 16 – The harvest omission rate and stem breaking rate of tobacco stems under different clamping chain gaps

As shown in Fig. 16, when the clamping chain gap was between 7 and 9 mm, the harvest omission rate decreased as the clamping chain gap increased. When the clamping chain gap was between 9 and 15 mm, the harvest omission rate increased as the clamping chain gap increased, reaching a maximum at 15 mm and then stabilizing. The stem-breaking rate decreased as the clamping chain gap increased. Therefore, the optimal clamping chain gap for the removal efficiency was 9–15 mm.

3.1.4. Analysis of Tobacco Stem Crushing Performance

The primary factors affecting tobacco stem crushing efficiency are the conveyor chain transmission speed and the cutting roller rotational speed *(Guo et al., 2023)*. The conveyor chain speed was set to 0.7 m/s, and the cutting roller rotational speed was set to 800 r·min^{-1}. For each test, a random sample of 100 crushed tobacco stems was selected for length measurement. The experiment was repeated three times, and the average value of the three measurements was calculated. The experimental test setup is shown in Fig. 17(a).

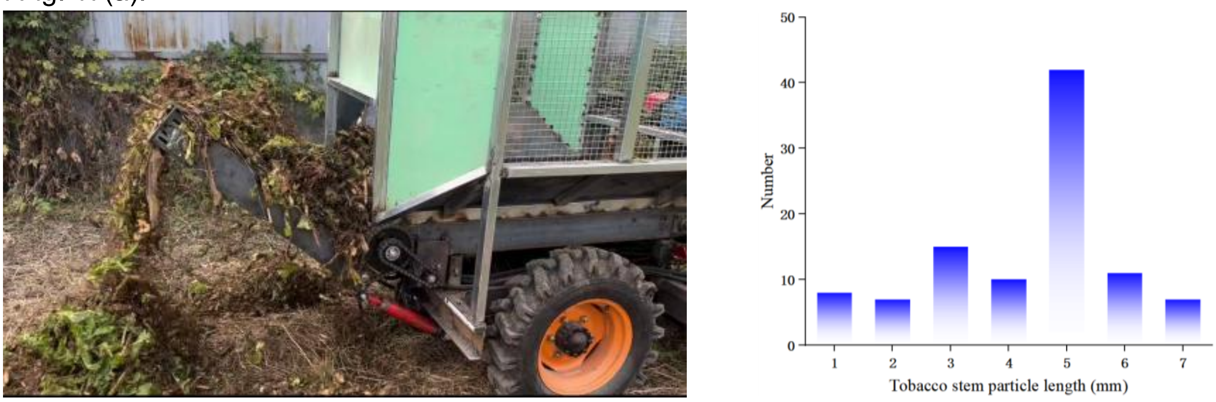

(a) Automatic unloading process of crushed tobacco stems

(b) Statistical distribution of tobacco stem crushing effectiveness

Fig. 17 – Tobacco stem crushing effectiveness

As shown in Fig. 17(b), the number of crushed tobacco stem particles was primarily concentrated in the 40–50 mm range, followed by the 20–40 mm and 50–70 mm ranges. No particles larger than 70 mm were observed, which generally aligns with a normal distribution. The crushing results met the design expectations.

3.2. Multi-factor orthogonal experiment

3.2.1. Experimental design

To analyse the interactive effects between the clamping chain speed, harvester forward speed, and clamping chain gap, a multi-factor orthogonal experimental design was developed based on single-factor experiments. The clamping chain transport speed was set to 0.6, 0.7, and 0.8 m/s, the forward speed of the tobacco stem harvester was set to 0.4, 0.5, and 0.6 m/s, and the clamping chain gap was set to 9, 12, and 15 mm. An $L_9(3^3)$ orthogonal array was employed, consisting of nine experimental runs, with the experimental scheme presented in Table 1.

Table 1

Table of orthogonal test protocols

Number	Forward speed (m/s)	Clamping chain transport speed (m/s)	Clamping chain gap (mm)
1	0.4	0.6	9
2	0.4	0.7	12
3	0.4	0.8	15
4	0.5	0.6	12
5	0.5	0.7	15
6	0.5	0.8	9
7	0.6	0.6	15
8	0.6	0.7	9
9	0.6	0.8	12

3.2.2. Test Results and Analysis

In each test group, 100 tobacco stems were pulled out, and the number of stems that were not pulled out and the number of broken stems were counted. The harvest omission and stem-breaking rates for each group were calculated, and the test results are presented in Table 2.

Table 2

Orthogonal test results

No.	Forward Speed (m/s)	Clamping Chain Transport Speed (m/s)	Clamping Chain Gap (mm)	Harvest Omission Rate (%)	Stem Breaking Rate (%)
1	0.4	0.6	9	6	10
2	0.4	0.7	12	4	2
3	0.4	0.8	15	12	2
4	0.5	0.6	12	8	6
5	0.5	0.7	15	14	2
6	0.5	0.8	9	10	16
7	0.6	0.6	15	12	4
8	0.6	0.7	9	8	18
9	0.6	0.8	12	10	6

Although orthogonal experiments can determine the optimal combination of working parameters for equipment field operations, it is difficult to intuitively quantify the extent to which travel speed, clamping chain speed, and clamp gap affect the harvest omission and stem breakage rates. Therefore, to accurately identify the significant differences between each factor and their impact on operational performance, it is necessary to further use the range analysis method to conduct an in-depth analysis of the experimental data. The results of the range analysis for the rate of harvest omission and stem breaking are shown in Tables 3 and Table 4.

Table 3

Range analysis of the harvest omission rate

Value	Forward Speed (m/s)	Clamping Chain Speed (m/s)	Clamping Chain Gap (mm)
K1	7.333	8.667	8.000
K2	10.667	8.667	7.333
K2	10.000	0.667	12.667.
Extreme Difference	3.334	2.000	5.334

Table 4

Range analysis of the stem breaking rate

Value	Forward speed (m/s)	Clamping chain speed (m/s)	Clamping chain gap (mm)
K1	4.667	6.667	14.667
K2	8.000	7.333	4.667
K2	9.333	8.000	2.667
Extreme difference	4.666	1.333	12.000

Different factors, levels, and response indicators yield varying effects, and a larger range value indicates a greater influence of a factor on the experimental results. As shown in Table 3, the order of influence of the factors on the harvest omission rate was clamping chain gap > forward speed > clamping chain speed. Similarly, as shown in Table 4, the order of influence of the factors on the stem breakage rate was clamping chain gap > forward speed > clamping chain speed.

Based on the analysis of the above experimental results, when the forward speed is 0.4 m/s, the clamping chain speed is 0.7 m/s, and the clamping chain gap is 12 mm, the comprehensive operational performance of the tobacco stem harvester is optimal.

4. CONCLUSIONS

This study focuses on the design and experimental research of a self-propelled tobacco stem harvester. The main design parameters of the self-propelled tobacco stem harvester were established through field testing of tobacco stems and soil physical properties, combined with literature analysis to determine key component parameters, and validated through simulation and field trials. The main conclusions are as follows.

(1) A chain-clamp-holding and transport device was designed, which integrated a spring-loaded clamping mechanism and hydraulic adjustment system to achieve a dynamic adaptive adjustment of the clamping gap. This effectively addresses issues such as slippage and missed extraction during tobacco stem transportation, significantly enhancing the harvesting reliability.

(2) Based on the Ansys static simulation analysis, the maximum stress of the soil loosening blade structure under operational conditions was 22.35 MPa, and the maximum deformation was 0.0125 mm, both of which were below the material's allowable strain value, thus verifying the structural strength and stability. Based on Adams' dynamic simulation results, the entire machine operated smoothly and met the design performance requirements.

(3) Through field single-factor experiments, the optimal parameter ranges were determined as follows: clamping chain transmission speed of 0.6–0.8 m/s, clamping gap of 9–15 mm, and harvester forward speed of 0.4–0.6 m/s. Further optimization through multi-factor orthogonal experiments yielded the optimal parameter combination: forward speed of 0.4 m/s, clamping chain transport speed of 0.7 m/s, and clamping chain gap of 12 mm. Crushing performance tests showed that the particle size of crushed tobacco stems was primarily distributed between 40 and 50 mm, with a size distribution conforming to a normal distribution pattern, achieving the design-expected crushing effect.

ACKNOWLEDGEMENT

This research was funded by the Key R&D and Promotion Special Tackling Key Problems in Science and Technology in Henan Province, China (grant no. 242102111173, 242102111172); Henan Province Tobacco Company Pingdingshan Company Science and Technology Project (PYKJ202204); Key Research Fund of Pingdingshan University (grant no. 2023-JYZD01).

REFERENCES

[1] Chen, T., Yi, S.J., Wang, S., Sun, W.S. (2025). Working Mechanism Analysis and Experimental Study of Grass Crusher. *INMATEH-Agricultural Engineering*, 75, 334-345. doi: https://doi.org/10.35633/inmateh-75-28.

[2] Fan, W. (2022). *Design and research on key components of Small Self-walking White Radish Harvester*, Guizhou University. doi: 10.27047/d.cnki.ggudu.2022.001679.

[3] Gao, S.B., Yuan Y.W., Niu, K., Zhao B., Zhou, L.M., Lv, C.X., Bai, S.H., Zhang, S.Y., An, R. (2025). Design And Experiment of Clamping and Conveying Device for Tracked Self-Propelled Chinese Cabbage Harvester. *INMATEH - Agricultural Engineering*, 1, 376-389. doi: https://doi.org/10.35633/inmateh-75-32.

[4] Guo, T.S., Zhang, Q., Wang, X., Yang, B.K., Yin, Z.C., Liu, H.X., Li, X., Ye, W.R., Cao, X.C., Luo, K.P., Shi, L. (2023). Current Situation and Development Suggestions of Tobacco Stalk Cleaning Machinery in China. *South Agricultural Machinery*, 12, 19-37+27. doi: 10.3969/j.issn.1672-3872.2023.12.005.

[5] Guo, T.S. (2023). Design and research on key components of tobacco straw cleaning machinery in field. *Yunnan Agricultural University*. doi: 10.27458/d.cnki.gynyu.2023.000636.

[6] Jin, B.H., Cha, Z.G., Chen, L., Jin, W.B. (1999). Study on the Extraction of Pectin from Tobacco. *Anhui Chemical Industry*, 3, 7-9.

[7] Jiang, Y.J., Liao, Y.T., Liao, Q.X. (2019). Design and Experiment on Cylinder-type Chopping Device of Harvester for Fodder Rapeseed in Winter and Spring. *Transactions of the Chinese Society for Agricultural Machinery*, 2, 102-111. doi: 10. 6041/j. issn. 1000-1298. 2019. 02. 011

[8] Li, X.W., Li, G.P. (1999). New Approaches to Industrial Utilization of Tobacco Stems. *China Dairy*, 4, 30-31.

[9] Li, J., Li, J.C., Wu, X.H., Zi, W.H., Yang, Y.F., Liu, Y.S. (2010). Progress in Research on Comprehensive Utilization of Tobacco Waste. *Yunnan Chemical Technology*, 2, 44-49. doi: 10.3969/j.issn.1004-275X.2010.02.010.

[10] Li, Y. (2009). Influence of Tobacco Plant Residues on the Occurrence of Diseases and Pests and Their Removal Measures. *XianDai NongYe KeJi*, 23, 182. doi: 10.3969/j.issn.1007-5739.2009.23.126.

[11] Mo, Z.J. (2023). *Study on the Formation Mechanism of Nicotine Transport Heterosis in Tobacco Hybrids*. Guizhou University. doi: 10.27047/d.cnki.ggudu.2023.000040.

[12] Pu, M.H. (2005). *The Virtual Design and Simulation for Small-Scale Type* [MA thesis]. Guangxi University.

[13] Reynaldo C.C., Shirley C.A., Julie L.L. (2000). Study on the Manufacture of Fiberboard from Tobacco Stalks. *Tobacco Science & Technology*, 7, 32-34. doi: 10.3969/j.issn.1002-0861.2000.07.015.

[14] Tu, J.H. (2006). *Study on Preparation and Characterization of Tobacco-stem-based Lignoceramics*. Kunming University of Science and Technology.

[15] Tong J, Moayad Z B. (2005). Effects of rake angle of chisel plough on soil cutting factors and power requirements: A computer simulation. *Soil & Tillage Research*, 1, 55-64.

[16] Wu, Z.L. (2007). *Purification and Some Properties of Sucrase from Tobacco (Nicotiana Tabacum L) Leaves*. Southwest University. doi: 10.7666/d.y1074057.

[17] Wang, W.J., Hu, Z. (2007). Agricultural Machinery Designing Handbook. *Beijing: Agricultural Science and Technology Press*.

[18] Yang, B., Sun, S.L., Li, J.Z., Zhang, W.J., Xun, Z.F. (2015). Design and Experiment for Stem Pulling and Stump Cutting Device of Tobacco Stem Pulling Machine. *Journal of Hunan Agricultural University (Natural Sciences)*, 4 446-449. doi: 10.13331/j.cnki.jhau.2015.04.021.

[19] Yu, Y.C., Liu, W.Y., Zhao, Y.F., Sun, J.Q. (2007). Force Mathematical Model and Examination Analysis of the Column Subsoiler. *Transactions of the Chinese Society of Agricultural Engineering*, 6, 109-113. doi: 10.3321/j.issn:1002-6819.2007.06.021.

[20] Yang, T.Y., Zhang, D.F., Shu, C.S., Yu, C.J., Cao, Y. (2024). Vibration Characteristics and Dynamic Analysis of Knife Roll of Tobacco Stalk Pulling and Crushing Machine. *Journal of Chinese Agricultural Mechanization*, 12, 9-14+29. doi: 10.13733/j.jcam.issn.2095-5553.2024.12.002.

[21] Zeng, J.J., Li, J.Z., He, W., Duan, M.Z., Peng, Z.G., Zhou, D.F. (2024). Analysis of the Current Status of Tobacco Fertilisation Machinery Research and Recommendations for Development. *Agriculture & Technology*, 6, 9-11, doi: 10.19754/j.nyyjs.20240330003.

[22] Zhang, J.F. (2016). An Analysis of the Impact of the Tobacco Industry on Local Economies Under Government Regulation. *China Market Marketing*, 50, 68+70. doi: 10.13939/j.cnki.zgsc.2016.50.068.

[23] Zhang, L.P. (2007). *Study on the Preparation of Tobacco-stem-based Activated Carbon and Its Adsorption Treatment of Heavy Metal-containing Wastewater* [PhD dissertation]. Kunming University of Science and Technology.

[24] Zhang, L. (2014). *Design of Chain-type Plastic Film Collector for Potato* [MA thesis]. Shandong Agricultural University.